

Tunable High-Q Photonic Band gap Cavity

Ankur Agrawal¹, Akash V. Dixit¹ David I. Schuster¹, and Aaron Chou²

¹ The University of Chicago, IL-60637, USA

² Fermilab National Laboratory, Chicago, IL-60637, USA
 ankuragrawal@uchicago.edu

Abstract. We present the design of a tunable high-Q photonic band gap (PBG) cavity, made from a periodic arrangement of dielectric rods in a woodpile like structure. We know that the axion signal rate diminishes as we move to higher axion mass searches. High quality factor achieved with this type of cavity will enable higher mass axion search with improved signal sensitivity and faster scanning rate. Quality factor in excess of the axion-Q will enable us to design interesting experiments such as the quantum non-demolition (QND) measurement of itinerant microwave photons using superconducting qubits, and stimulated emission of photons.

Keywords: photonic bandgap, dark matter axion, microwave cavity.

1 Introduction

A woodpile structure made out of dielectric rods exhibits an omnidirectional photonic bandgap (PBG) which forbids the propagation of electromagnetic wave with energy within a certain range in all directions. We designed an electromagnetic cavity by creating a defect inside the crystal, such that its frequency lies within the forbidden bandgap. Very high Q-factors can be achieved since the light has no way to escape because of the bandgap and is only limited by the dielectric loss in the material. We predict the quality factor of such a cavity to be close to 10^8 near 10 GHz. The cavity frequency is tuned by sliding the rods in and out. One of the potential applications is in the axion dark matter search, which is currently limited by the use of low Q-factor copper cavities due to the presence of a strong magnetic field. We predict the Q-factor of a PBG cavity to increase in the presence of a large magnetic field due to the shift in the two-level system energies to a higher level.

2 Photonic Bandgap

The control of electric currents achieved with the semiconductors such as silicon is dependent on a phenomenon called the bandgap: a range of energies in which the electron is blocked from travelling through the semiconductor. Scientists have produced material with a photonic bandgap- a range of wavelengths of light which is blocked by the material. The analogy between electron-wave

propagation in real crystals and the electromagnetic-wave propagation in a multidimensionally periodic structure has proven to be a fruitful one. It allows us to manipulate light in addition to electric currents. Photonic crystals occur in nature in the form of structural coloration and animal reflectors as shown below. The existence and properties of an electronic bandgap depend crucially on the

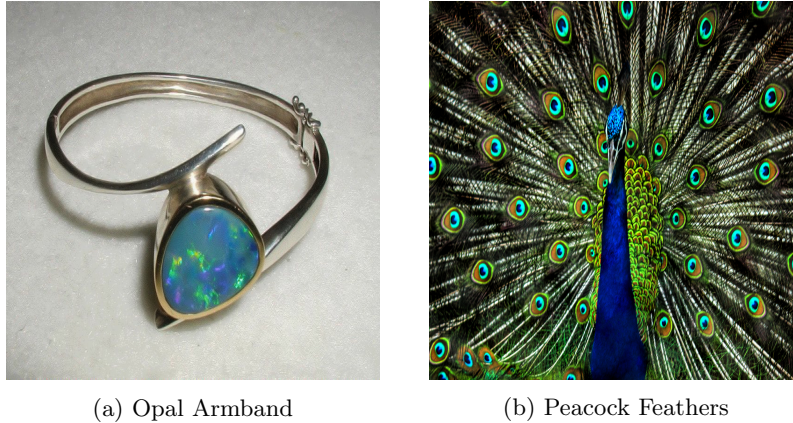


Fig. 1: Natural periodic micro-structures responsible for the iridescent color in stones and feathers (Source: Wikipedia).

type of atoms in the material and their crystal structure - spacing between the atoms and the shape of the crystals they form. In the *optical* analogue, atoms or molecules are replaced by macroscopic media with differing dielectric constants, and the periodic potential is replaced by the periodic dielectric function.

3 Photonic Bandgap Crystal

The simplest photonic bandgap material is the periodic arrangement of alternating layers of materials with different dielectric constants. In a 1-dimensional photonic crystal, the band-stop edges are determined by the frequency of the waves propagating in the dielectric band and the air band, given by $f_{\text{air}} = \frac{c}{\lambda_0}$ and $f_{\text{diel}} = \frac{c/n_{\text{diel}}}{\lambda_0}$ respectively. It has been shown that the size of the band-gap increases with the increase in dielectric contrast, and it reaches a maximum at an optimal volume filling fraction [1].

The presence of an omni-directional band gap in the 3D woodpile structure was demonstrated early [1], and the defect cavity modes within the bandgap were well studied. In recent experiments, nanocavities created inside the woodpile crystals made out of semiconducting material have achieved Q's as high as 38,500 at 4K [2]. These Q-values are already high compared to the copper cavities which

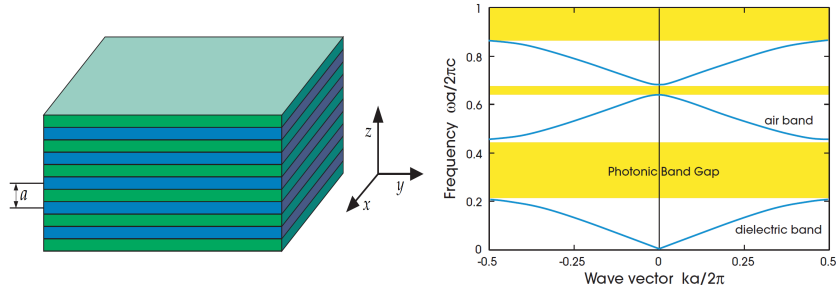


Fig. 2: (Left) The multilayer films, a one-dimensional photonic crystal. The system consists of alternating layers of materials with different dielectric constants, with a spatial period of a . (Right) The photonic band structure of a multilayer-film with lattice constant a and alternating layers of different widths. The width of the $\epsilon = 13$ layer is $0.2a$ and the width of the $\epsilon = 1$ layer is $0.8a$ [3]

can achieve $Q \sim 10^4$ at 10 GHz at 20 mK.

Inspired by these results, we constructed the woodpile structure using commercially available alumina bars. The woodpile structure is assembled by stacking together layers of dielectric rods, with each layer consisting of parallel rods with a center-to-center separation of d . The rods are rotated by 90° in each successive layer. Next, the rods in third and fourth layers are displaced by a distance of $0.5d$ perpendicular to the first and the second layer respectively, as shown in Fig.3. This results in a face-centered-tetragonal (fct) symmetry where each unit cell repeats after four layers. We kept the separation, $d = a/\sqrt{2}$ and the width and the height of bars to be $0.25a$ ($w = h = 0.25a$).

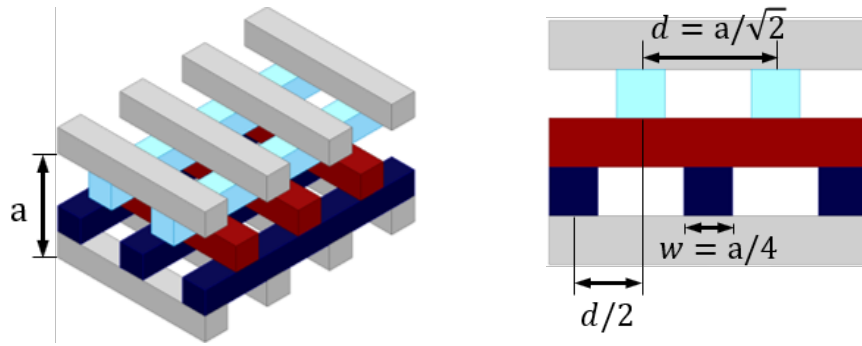


Fig. 3: (Left) Isometric view of the unit cell. (Right) Front view of the unitcell depicting all the lattice parameters.

We simulated a 3D woodpile structure using the **MIT mpb** simulation package [4] to determine the optimal lattice parameters. The simulation predicts a complete band gap of 14.24 % at the center frequency as shown in the band-structure diagram in Fig. 4. The band-stop edges are given by $0.490 \frac{c}{a}$ and $0.562 \frac{c}{a}$ (9.5 GHz-11.1 GHz), where a is the periodicity along the stacking direction. We measured the transmission spectra using a Vector Network Analyzer. The cables were calibrated up to the ends of the dipole antennae. The measured transmission spectra is shown in the Fig.4 where the bandgap lies between 9.5 GHz and 11.1 GHz, which agrees well with the simulation result. We varied the power incident on the crystal to check if the lowest level of the transmission in the bandgap is limited by the noise floor of the VNA and we didn't observe any change in the lowest level, implying the lowest level is indeed the suppression in transmission. Further, the entire structure was covered with ECCOSORB sheets to provide absorbing boundary condition at the surface and suppress any direct coupling between the antennae. The experimental set-up is presented in Fig. 5.

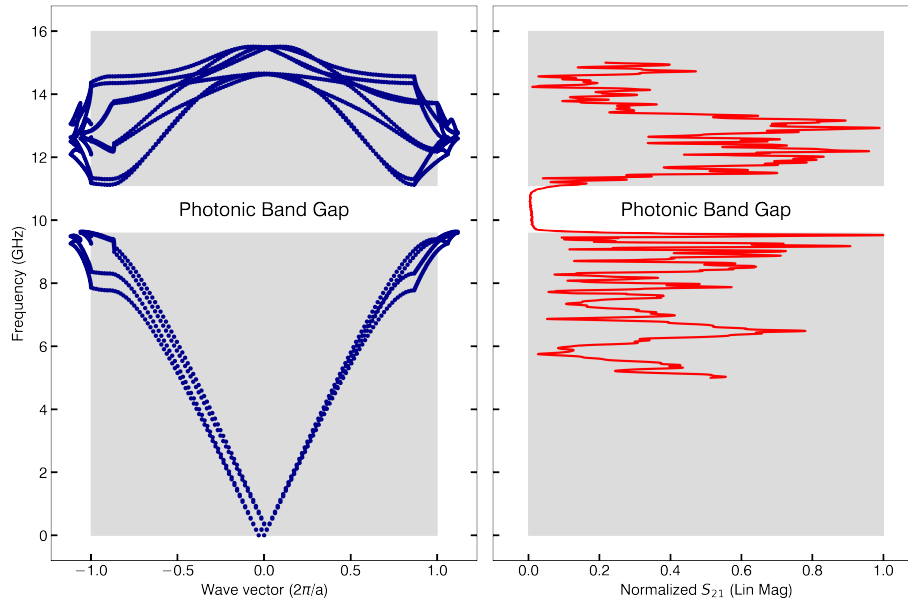


Fig. 4: (Left) The photonic band structure for the lower bands of a woodpile structure simulated using mpb. (Right) Measured transmission S_{21} through the woodpile photonic crystal; bandgap of 1.6 GHz centered around 10.3 GHz

4 Photonic Bandgap Cavity

The defect state within the bandgap is created by either removing material or by adding material to the crystal.

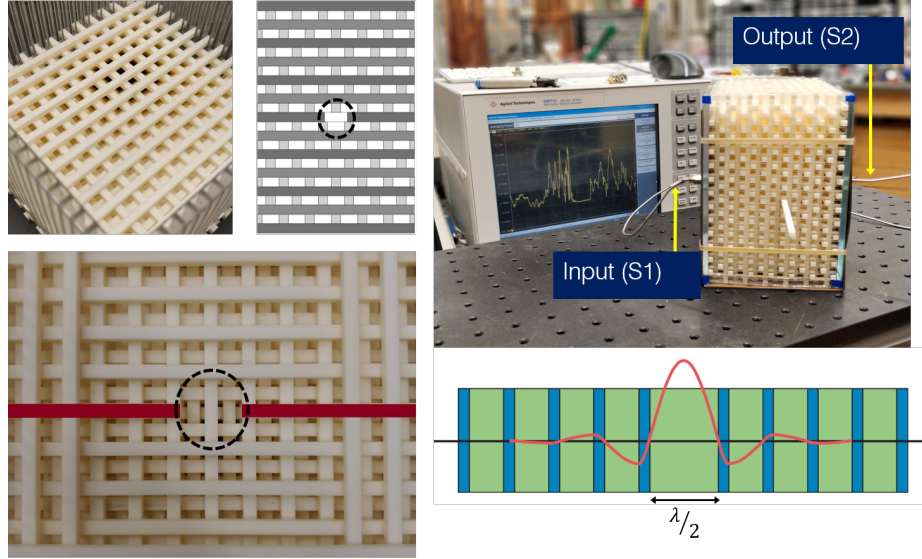


Fig. 5: (Left column) The assembled woodpile PBG crystal. Defect layer shown in the front and top view. (Right) The experimental apparatus showing the input-output ports connected to a VNA. (Right-bottom) The exponential attenuation of the electric field as it enters the crystal [3]

We studied the variation of Q_i as a function of the cavity frequency within the bandgap. We observed that the Q_i reaches a maximum value at the center of the bandgap as seen in Fig. 7. It is reasonable to expect this hump in the center since the field will be attenuated maximally.

4.1 Estimation of Field Attenuation

To maximally utilize the space inside a magnet bore, we need to estimate the number of periods required to attenuate the field such that the quality factor is not limited by the boundary condition. We know that the loss rate due to multiple decay mechanisms is given by,

$$\kappa = \kappa_1 + \kappa_2 + \dots \quad (1)$$

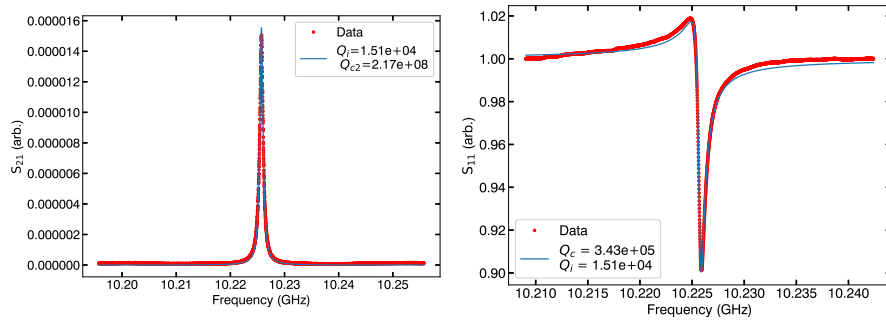


Fig. 6: (Left) Transmission (S_{21}) spectra of the defect cavity. (Right) Reflection (S_{11}) spectra of the defect cavity.

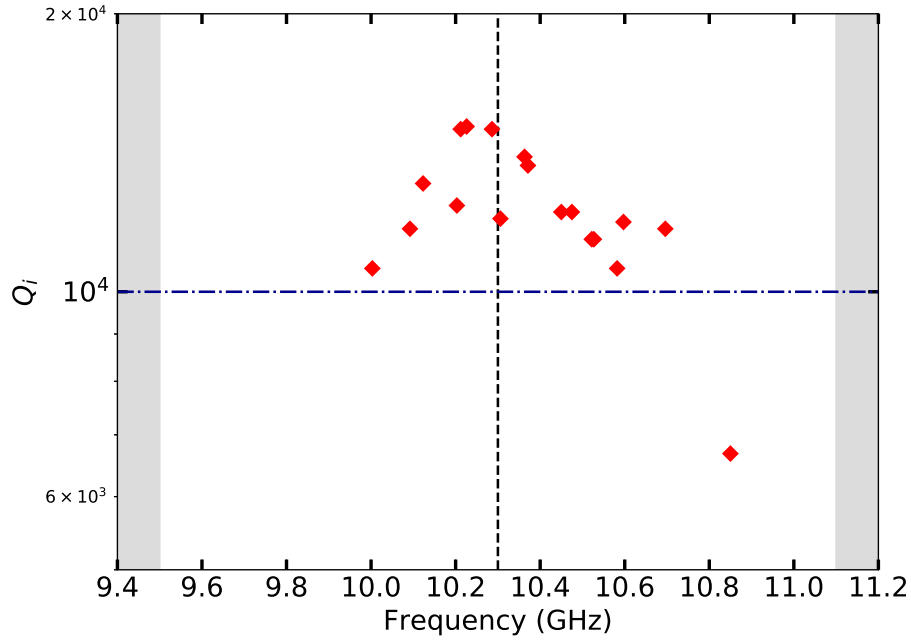


Fig. 7: Variation of the internal quality factor, Q_i as a function of the defect frequency in the bandgap. Blue dashed line represents the quality factor of a 10 GHz copper cavity at 20 mK.

where κ is the total loss rate. The internal quality factor, Q_i is related to the dielectric (Q_d), conductor (Q_c), and radiation losses (Q_r) by

$$\kappa = \frac{1}{Q} = \frac{1}{Q_d} + \frac{1}{Q_c} + \frac{1}{Q_r} \quad (2)$$

The power loss in the conductor is proportional to the square of the surface current [textbook] such that the loss is proportional to the square of the magnitude of the field at the boundary

$$P_c \propto J^2 \propto H(r)^2 \quad (3)$$

and, the power loss in a dielectric material is given by its loss tangent which would maximally be limited by the fraction of field residing inside the lossy dielectric material

$$Q_d = \frac{1}{\tan(\delta)} \quad (4)$$

In summary, the total loss rate is given by

$$\kappa = w_c \kappa_c + w_d \kappa_d + w_r \kappa_r \quad (5)$$

where, w_c , w_d and w_r are the participation ratios of the mode in the dielectric, conductor, and radiation.

5 Conclusion

We have demonstrated a complete bandgap in the woodpile like photonic crystal. The defect-cavity Q-factor measured at room temperature is higher than the copper cavity at 20 mK, which is promising. At cryogenic temperature, we expect to see an improvement in the Q-factor by at least an order of magnitude. Ultimately, we would like to construct this PBG cavity using high purity Sapphire ($\tan(\delta) \sim 10^{-8} - 10^{-9}$ at 27 mK at 13 GHz)[5] to achieve Q-factors higher than 10^8 . It will hugely impact the axion search by improving the scanning rate to a factor of $\frac{Q_i}{10^4}$. In other words, for a $Q_i = 10^6$ we can scan the axion mass range 100 times faster than the current technology.

6 Acknowledgements

This research was supported by the Heising-Simons Foundation. We would like to thank Steven G. Johnson for simulation scripts and helpful discussion. This manuscript has been authored by Fermi Research Alliance, LLC under Contract No. DE-AC02-07CH11359 with the U.S. Department of Energy, Office of Science, Office of High Energy Physics.

References

- ¹K. M. Ho, C. T. Chan, and C. M. Soukoulis, “Existence of a photonic gap in periodic dielectric structures”, *Phys. Rev. Lett.* **65**, 3152–3155 (1990).
- ²A. Tandraechanurat, S. Ishida, D. Guimard, M. Nomura, S. Iwamoto, and Y. Arakawa, “Lasing oscillation in a three-dimensional photonic crystal nanocavity with a complete bandgap”, *Nature Photonics* **5**, 91 (2011).

- ³J. D. Joannopoulos, S. G. Johnson, J. N. Winn, and R. D. Meade, *Photonic crystals molding the flow of light* (Princeton University Press, 2017).
- ⁴S. Johnson and J. D. Joannopoulos, “Block-iterative frequency-domain methods for maxwell’s equations in a planewave basis”, *Opt. Express* **8** (2001).
- ⁵D. L. Creedon, Y. Reshitnyk, W. Farr, J. M. Martinis, T. L. Duty, and M. E. Tobar, “High q-factor sapphire whispering gallery mode microwave resonator at single photon energies and millikelvin temperatures”, *Applied Physics Letters* **98**, 222903 (2011).